

Miniature Printed Magnetic Photonic Crystal Antennas Embedded into Vehicular Platforms

Erdinc Irci, Kubilay Sertel, and John L. Volakis

ElectroScience Laboratory, Department of Electrical & Computer Engineering
The Ohio State University, 1320 Kinnear Rd. Columbus, OH 43212, USA
ircie@ece.osu.edu, sertel@ece.osu.edu, volakis@ece.osu.edu

Abstract - In this paper, a miniature printed antenna utilizing magnetic photonic crystal (MPC) modes is presented. Typically, MPC modes are supported by a combination of anisotropic dielectric and ferrimagnetic layers. Here, these modes are emulated using coupled printed lines on a grounded dielectric substrate with small, biased ferrimagnetic inclusions. The resonant antenna is formed by cascading two unit cells excited with a probe feed. A recessed, cavity-backed version of this antenna is embedded into a vehicular platform with a goal to minimize platform effects. Several locations on the vehicle are studied and antenna placement is optimized using a combination of two commercially available electromagnetic simulators.

Index Terms - Anisotropic media, coupled microstrip lines, degenerate band edge (DBE) crystals, magnetic photonic crystals (MPC), metamaterials, miniature antennas, embedded antennas, vehicular antennas.

I. INTRODUCTION

Conventional military ground vehicles usually end up being populated with many protruding antennas, making them vulnerable targets. Thus, when installing antennas on such vehicular platforms, a typical objective is to reduce their profile and decrease their radar signature, while maintaining the performance delivered by protruding antennas. However, for multipurpose military ground vehicles, antenna installation is even more challenging due to

limited areas for placement. More specifically, the large conducting surfaces found on the hood and roof cannot be used due to other utilities (such as weapon installments, spare tires, supplies, and personnel transportation). Therefore, antennas need be placed (still conformally) towards the edges of vehicle roof, doors, bumpers, and windows frames. These restrictions place additional challenges for designing antennas that are less susceptible to nearby structure effects. Such platform effects must be reduced to suppress the need for antenna retuning when installed. In this paper, we introduced a cavity-backed (slot type) antenna that remains stable even when placed within 1.5" (3.81cm) of the vehicle's edges.

The proposed miniature antenna is based on modes found in periodic stacks of misaligned dielectric layers, similar to those shown in Fig. 1(a)-left. These novel modes were referred to as degenerate band edge (DBE) and magnetic photonic crystal (MPC) modes [1-3]. Extreme wave slow down at much lower frequencies was harnessed for realizing miniaturized and highly directive antennas [4-6]. More recently, the misaligned anisotropic dielectric layers in these volumetric crystals were successfully emulated by a combination of uncoupled and coupled microstrip line sections on uniform substrates; see Fig. 1(a)-right. The DBE modes emulated using such coupled lines enabled miniature, high gain microstrip antennas [7]. Specifically, the maximally flat dispersion curves of DBE crystals, shown in Fig. 1(b)-left, allowed for significant miniaturization over microstrip loop

and patch antennas. However, the zero slope associated with the $K = \pi$ resonance at the band edge suffers from reduced bandwidth. As a remedy, in this paper we introduce biased ferrimagnetic inclusions at the coupled line

sections to obtain nonreciprocal MPC dispersion modes. As depicted in Fig. 1(b)-right, nonzero slope is realized in the dispersion curve around $K = \pi$ point. This implies improved miniaturization and bandwidth enhancement.

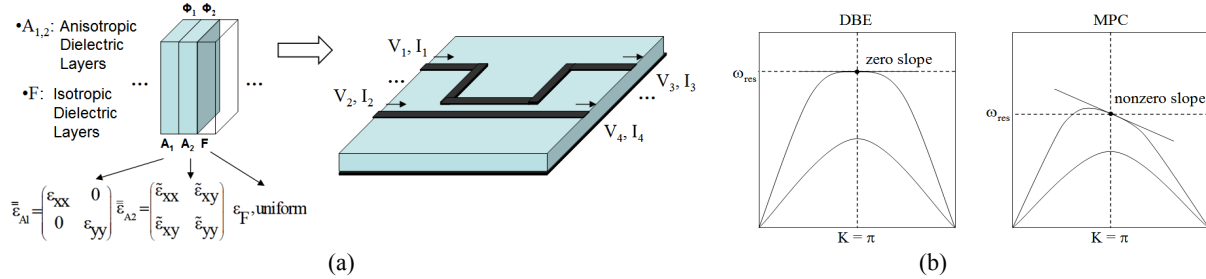


Fig. 1. (a) Coupled lines emulating anisotropy in a DBE unit cell. (b) DBE and MPC dispersion diagrams.

II. MPC ANTENNA DESIGN AND PERFORMANCE

Previously, DBE dispersion modes were emulated in [7] using uncoupled and coupled line sections on a uniform dielectric substrate, as shown in Fig. 2(a)-top. The uncoupled sections were bent inwards to attain a compact footprint. For emulating nonreciprocal MPC modes, small biased ferrimagnetic inclusions were inserted under coupled line sections, as depicted in Fig. 2(a)-bottom [8]. The corresponding dispersion curves of these DBE and MPC unit cells are shown in Fig. 2(b). Next, DBE and MPC antennas were formed by circularly cascading two unit cells, as depicted in Fig. 3(a). A coaxial probe feed and a small microstrip stub were also used to capacitively excite these DBE and MPC elements. As illustrated in Fig. 3(b), for the MPC case, ferrimagnetic inclusions under the coupled lines extend down to ground plane level and small magnets placed underneath provide the necessary DC magnetic bias. A rectangular patch antenna was also designed for comparison purposes. In all antennas, the same $2'' \times 2'' \times 0.5''$ ($5.08\text{cm} \times 5.08\text{cm} \times 1.27\text{cm}$) dielectric substrates with $2'' \times 2''$ ($5.08\text{cm} \times 5.08\text{cm}$) ground planes were used. MPC antenna in Fig. 3(a) with $0.8'' \times 0.87''$ ($2.03\text{cm} \times 2.21\text{cm}$) footprint resonates at 2.35 GHz, having 8.8% bandwidth and 6.2 dB realized gain. DBE antenna with a $0.97'' \times 0.99''$ ($2.46\text{cm} \times 2.51\text{cm}$) footprint resonates at the same frequency, having 6.9% bandwidth and 6.5

dB gain. Patch antenna at the same frequency has 11.6% bandwidth and 6.7 dB gain, by utilizing a much larger footprint of $1.23'' \times 1.14''$ ($3.12\text{cm} \times 2.9\text{cm}$). Hence, MPC antenna is 28% smaller than the DBE and 50% smaller than the patch (in terms of footprint area). Although much smaller in footprint size, MPC antenna maintains almost same bandwidth and gain as the patch. The substantial footprint reduction obtained by the MPC antenna suggests that its substrate size can be further reduced without much degradation in performance. This is explored in the next section when a cavity-backed configuration is considered.

A prototype of the MPC antenna in Fig. 3(a) was also fabricated and is shown at the inset of Fig. 4(a). The antenna substrate was formed using four layers of 125 mil thick Rogers Duroid 5880 dielectrics and was fastened using two plastic ribbons. The ferrimagnetic insertions (NG-1001 CVG of TCI Ceramics: $4\pi M_s = 976\text{G}$, $\Delta H = 70\text{e}$, $\epsilon_r = 14.2$ and $\tan\delta_d = 1 \times 10^{-4}$) were inserted into two rectangular holes in each dielectric layer. To bias the antenna, two small permanent magnets ($1'' \times 1/2'' \times 1/16''$: $2.54\text{cm} \times 1.27\text{cm} \times 1.59\text{mm}$) were placed underneath the ground plane. Its measured return loss is plotted in Fig. 4(a). As seen, this prototype delivered 9.1% bandwidth around 2.35 GHz and showed very good agreement with the 8.8% computed bandwidth at around the same frequency.

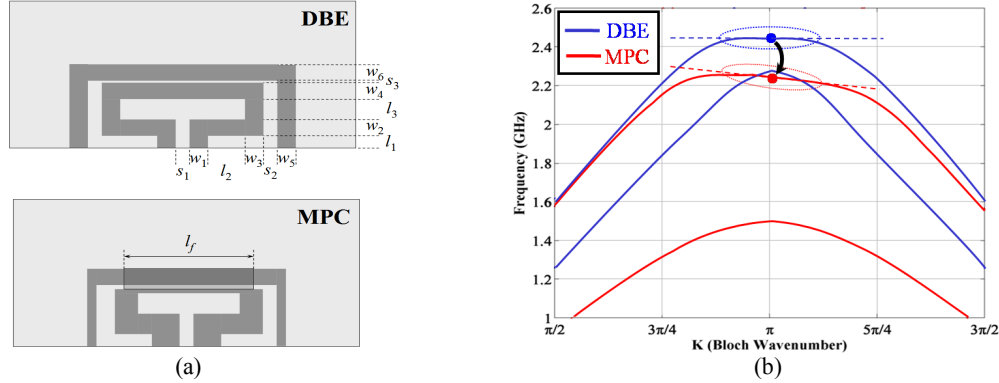


Fig. 2. (a) Layout of DBE and MPC unit cells. (b) DBE and MPC dispersion diagrams.

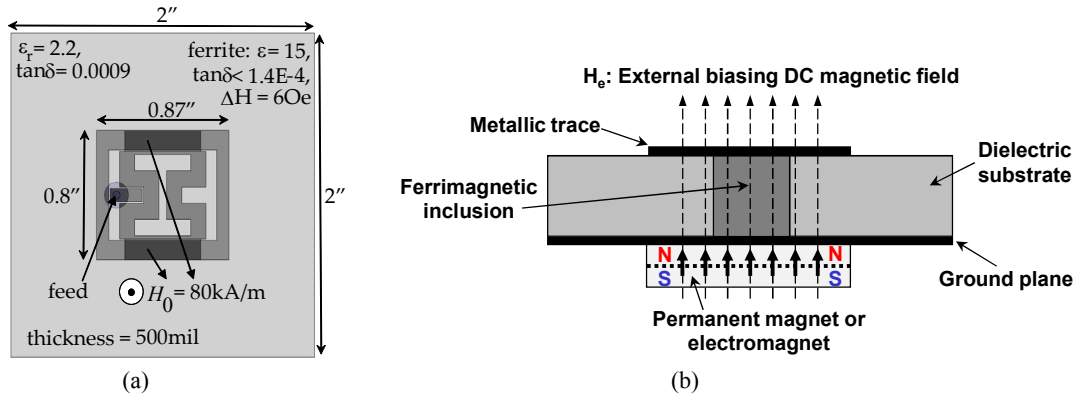


Fig. 3. (a) Resonant MPC antenna formed by circularly cascading two unit cells. (b) Practical realization of MPC modes using ferrimagnetic inclusions and DC magnetic bias.

The broadside realized gain of the fabricated MPC prototype was measured in the anechoic chamber. From Fig. 4(b), we observe a peak realized gain of 4.5 dB (70% efficiency) at 2.35 GHz. This is 1.3 dB smaller than the 5.8 dB computed gain (90% efficiency), which included all magnetic, dielectric and conductivity losses. This difference is attributed to non-uniform bias field inside the ferrimagnetic inclusions. The measured 4.5 dB realized gain is obtained when the MPC is in receiving (Rx) mode. Due to nonreciprocal behavior, its gain is 3.5 dB in transmit (Tx) mode. An opposite nonreciprocal behavior (i.e. Rx = 3.5dB, Tx = 4.5dB) is obtained by reversing the polarization of DC magnetic bias, show in Fig. 4b-left, top.

The realized gain of the unbiased MPC antenna (in the absence of biasing magnets, shown in Fig. 4b-left, bottom) was also measured. As seen in Fig. 4(b), the unbiased MPC has -1.25 dB gain at 2.35 GHz, which is 5.75dB less than the biased case. This

demonstrates that the MPC can be effectively switched on/off by toggling the magnetic bias.

III. CAVITY-BACKED MPC ANTENNA

Next, we considered a $1.5'' \times 1.5'' \times 0.5''$ ($3.81\text{cm} \times 3.81\text{cm} \times 1.27\text{cm}$) substrate. In addition, the MPC antenna is recessed below the ground plane by embedding it in a metallic cavity, as shown in Fig. 5(a). Consequently, a small and zero-profile aperture is created on the ground plane. The small size and flush mounting of the MPC antenna makes it suitable for installation at corners, edges, and vertical surfaces of the vehicle, while it is less susceptible to nearby effects. Since the ground plane sizes at such locations are varying, one undesirable effect is detuning of antenna resonance. We note that the recessed MPC antenna also mitigates such platform loading effects. When a $3'' \times 3''$ ($7.62\text{cm} \times 7.62\text{cm}$) ground plane is used, the MPC antenna resonates at 2.45 GHz with 3% bandwidth. As the ground plane size is made

much larger (e.g., $10'' \times 10'' = 25.4\text{cm} \times 25.4\text{cm}$ or infinite), the resonance slightly shifts to 2.42 GHz, while still keeping the 3% bandwidth, see Fig. 6 (a). In addition, these small detunings can be prevented by slightly tuning the magnetic bias, see Fig. 6 (b). For all cases, the broadside radiation pattern of the antenna is retained

almost the same, as can be observed from Fig. 5 (b). The main differences in radiation patterns are observed in back lobes, which are small. With this cavity-backed design, we next proceed to investigate the antenna performance on a representative automobile platform.

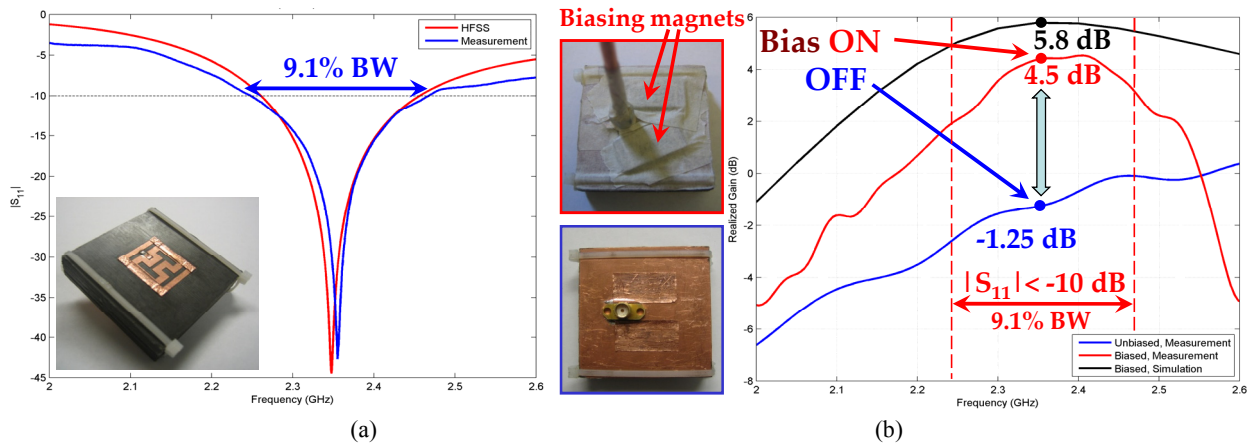


Fig. 4. Measured return loss and realized gain of the MPC antenna prototype in Fig. 3(a). (a) Return loss. (b) Realized gain at broadside.

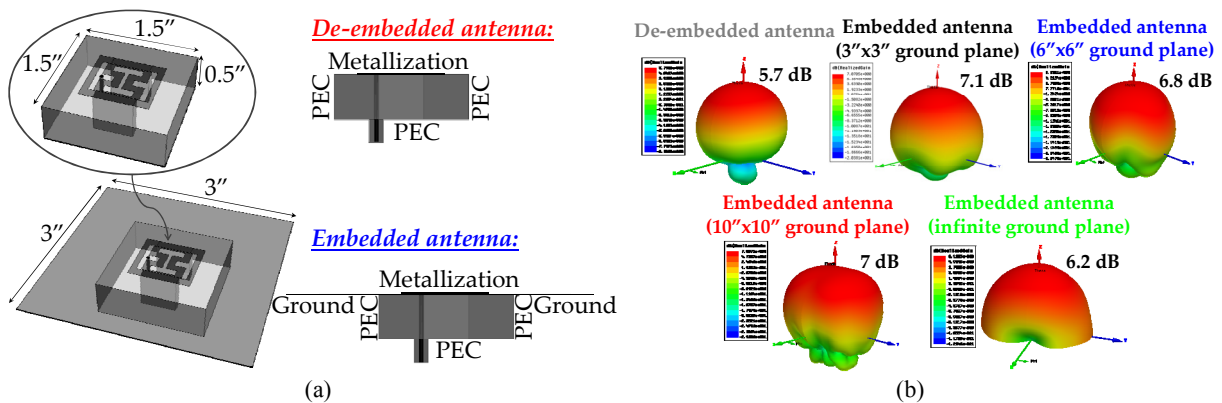


Fig. 5. (a) Cavity-backed (de-embedded) and recessed (embedded) MPC antenna geometries. (b) Radiation patterns of these MPC antennas.

IV. ANTENNA PLACEMENT ON REPRESENTATIVE AUTOMOBILE PLATFORM

To investigate the in-situ performance of the recessed MPC antenna, several locations on horizontal and vertical surfaces of the automobile platform were selected for antenna placement, as shown in Fig. 7(a). These included centers, edges, and corners of any large/small, horizontal/vertical surfaces. Since the MPC antenna incorporates biased ferrimagnetic

inclusions (with gyrotropic permeability tensors), it was designed using Ansoft HFSS. To analyze antenna placement on the electrically large vehicle, we used the uniform theory of diffraction (UTD) package of EMSS FEKO. To do so, the radiation pattern of the MPC antenna with $3'' \times 3''$ ($7.62\text{cm} \times 7.62\text{cm}$) ground was first obtained from HFSS. Then, this pattern was used as an excitation to illuminate the vehicle modeled using flat surfaces. Resulting radiation

patterns are given in Fig. 7(b)-(e). In all cases, a similar broadside radiation pattern is retained with a gain higher than 5.4 dB. Small ripples in the patterns can be observed when antennas are placed towards surface centers. This is due to different phase terms of diffraction contributions

from surface edges and their interference. These ripples are mostly avoided when the antenna is placed close to edges or corners of the surfaces, and overall gains are much improved in these cases.

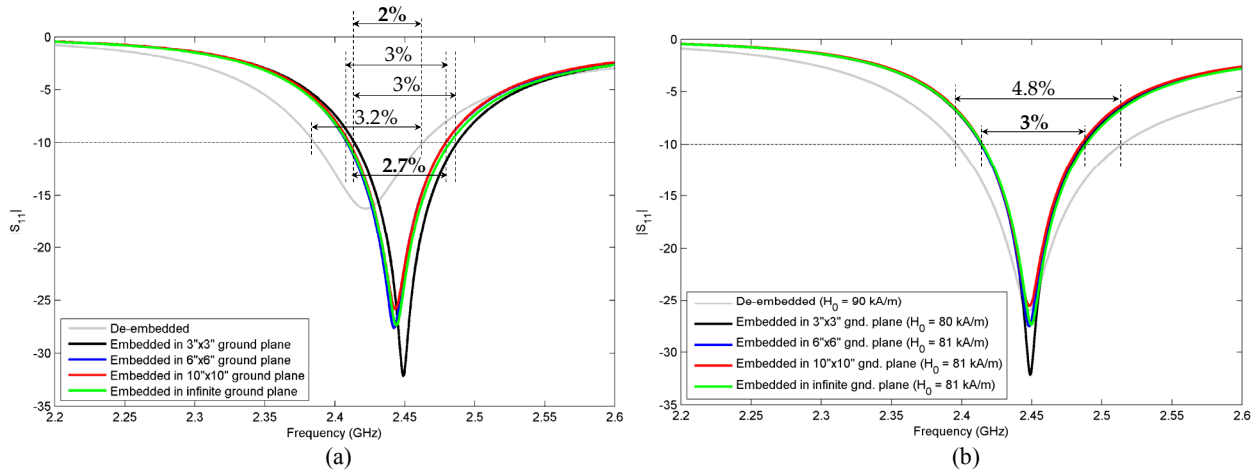


Fig. 6. (a) Return losses of cavity-backed MPC antennas recessed into a ground plane. (b) Return losses of cavity-backed and recessed MPC antennas after retuning magnetic bias.

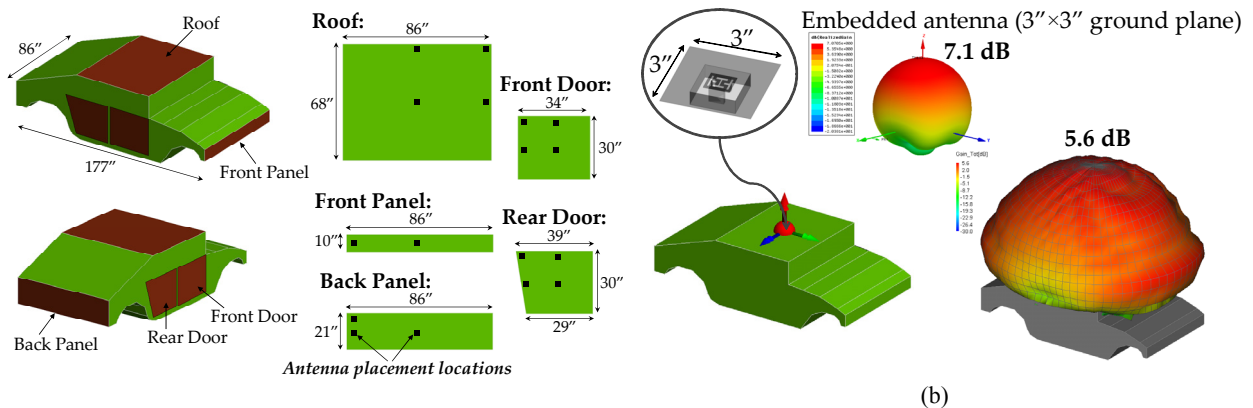
V. CONCLUSIONS

In this work, MPC modes were emulated and exploited for realizing smaller printed antennas with much improved bandwidths. Even smaller and cavity-backed versions of these antennas were embedded into a large vehicle. This resulted in zero-profile antennas and mitigated the platform loading effects, such as detuning of resonance or variations in radiation pattern. It is also found that these antennas would be suitable to be used much closer to the edges or corners of the vehicle for resulting in smaller ripple in patterns and improved gain. The presented design also alleviates the

restrictions of available areas for antenna placement by utilizing edges and corners on the vehicle body.

ACKNOWLEDGMENTS

This work was supported by the U.S. Air Force Office of Scientific Research under Grant FA9550-04-1-0359, Lockheed Martin Corporation Strategic Technology Threads Program, the U.S. Army Research Laboratory, Adelphi MD (through Applied EM Inc. under contract #W911QX-09-C-0017), and by The Ohio State University Research Foundation.



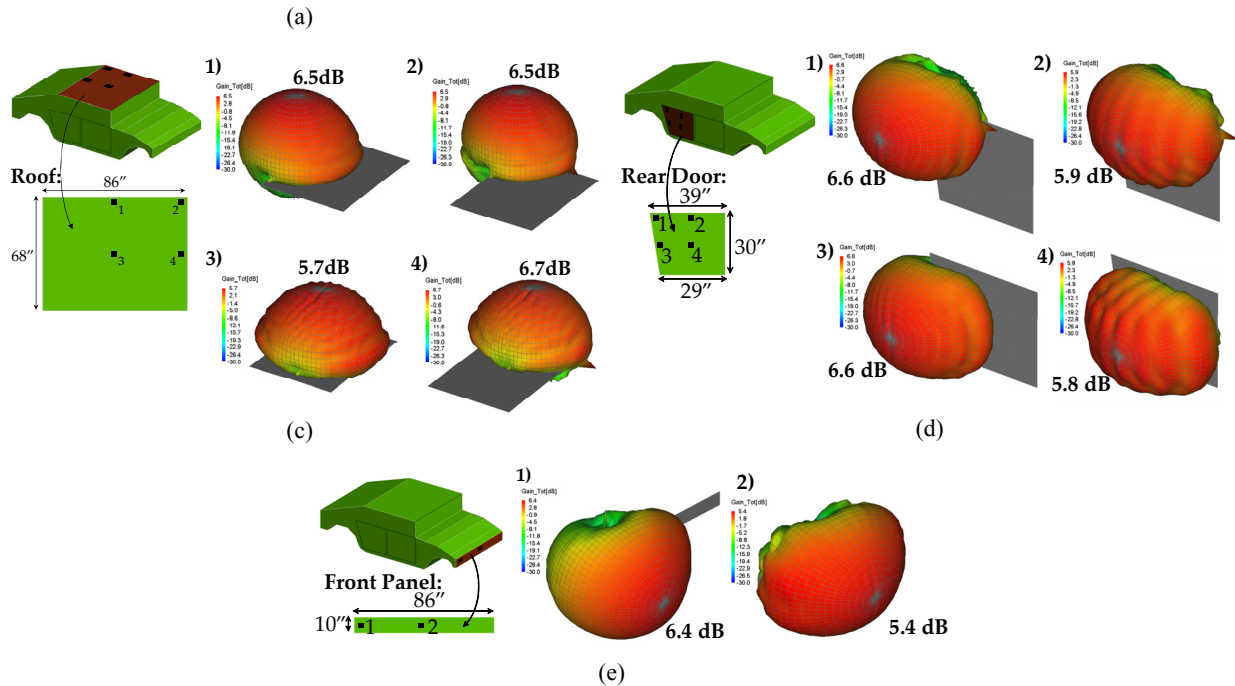


Fig. 7. (a) Selected antenna placement locations on the representative automobile platform. (b) Placement of recessed MPC antenna on the automobile platform. (c) Antenna placement at several locations on the roof, (d) rear door, and (e) front bumper.

REFERENCES

- [1] A. Figotin and I. Vitebsky, "Nonreciprocal Magnetic Photonic Crystals," *Phys. Rev. E*, vol. 63, pp. 066 609-066 625, Feb. 2001.
- [2] A. Figotin and I. Vitebsky, "Frozen Light in Photonic Crystals with Degenerate Band Edge," *Phys. Rev. E*, vol. 74-066613, pp. 1-17, Oct. 2006.
- [3] A. Figotin and I. Vitebsky, "Slow-Wave Resonance in Periodic Stacks of Anisotropic Layers," *Phys. Rev. E*, vol. 76-053839, pp. 1-12, Nov. 2007.
- [4] G. Mumcu, K. Sertel, and J. L. Volakis, "Miniature Antennas and Arrays Embedded within Magnetic Photonic Crystals," *IEEE Antennas Wireless Propag. Lett.*, vol. 5, pp. 168-171, Dec. 2006.
- [5] S. Yarga, G. Mumcu, K. Sertel, and J. L. Volakis, "Degenerate Band Edge Crystals and Periodic Assemblies for Antenna Applications," in *Proc. IEEE Int. Workshop on Antenna Technol. Small Antennas and Novel Metamater.*, pp. 408-411, Mar. 2006.
- [6] J. L. Volakis, K. Sertel, and C. C. Chen, "Miniature Antennas and Arrays Embedded within Magnetic Photonic Crystals and Other Novel Materials," *Applied Computational Electromagnetics Society Journal, Special Issue on ACES 2006 Conference*, vol. 22, no. 1, pp. 22-30, March 2007.
- [7] G. Mumcu, K. Sertel, and J. L. Volakis, "Miniature Antenna using Printed Coupled Lines Emulating Degenerate Band Edge Crystals," *IEEE Trans. Antennas Propag.*, vol. 57, no. 6, pp. 1618-1624, June 2009.
- [8] E. Irci, K. Sertel, and J. L. Volakis, "Antenna Miniaturization using Coupled Microstrip Lines Emulating Magnetic Photonic Crystals," in *Proc. 2009 IEEE Antennas and Propagation Soc. Int. Symp.*, pp. 1-4, 2009.